Journal of Civil Engineering and Urban Planning (2023)
Clausius Scientific Press, Canada

DOI: 10.23977/jceup.2023.050802
ISSN 2616-3969 Vol. 5 Num. 8

Optimized Design of Hydrodynamic Enhanced Water Pump System in Landscape Water System

Cheng Bi, Lin Tang, Guangming Mu, Yuancai Ma, Ziyang Mi, Weicong Cui, Xintao Shao, Ruibo Wang, Xidong Ding, Jun Cheng

Power China Railway Construction Investment Group Co. Ltd, Beijing, China

Keywords: Landscape water; Hydrodynamic drive method; Hydrodynamic model; Velocity

Abstract: In view of the small flow rate, slow velocity and closed circulation of landscape water, water quality deterioration is easy to occur, the hydrodynamic driving method is selected to treat landscape water. Based on hydrodynamic model, three cases were studied for optimal designing. Scheme 1 and 2 are boundary water inlet and outlet, scheme 3 is internal point water inlet and outlet. Analyze the flow rate of the three schemes, and choose the best scheme more intuitively. In Scheme 1, about 30% of the simulated flow area in the south region has a flow velocity exceeding 0.3m/s. About 50% of the flow rate in the northern region obtained by the simulation of Scheme 3 is greater than 0.30 m/s. By comprehensive comparison, it can be seen that the north region selection scheme 3 and the south region selection scheme 1 have the best effect on the overall flow velocity improvement and can be used as the best scheme.

The water quality problem of urban landscape water body has attracted a lot of attention, so the water quality conditions should be considered in the design of landscape water body to facilitate the maintenance of water quality after completion[1]. Su Lifeng[2]The application of micro-nano bubble technology in landscape water treatment is discussed: Wu Guorong[3]The method of treating high standard landscape water is proposed by Gao Wenqi[4]The application of micro-flocculation filtration process in building landscape water treatment is studied; Hu Zhongbang[5]The application of embedded control system in landscape water treatment is discussed[6]Analysis and application of landscape water treatment of nano-activated carbon fiber are proposed[7]The application of EW-MP microbial purification ecological water treatment system in the field of landscape water treatment was studied, but the above treatment method is too expensive and is not the optimal choice. This paper selects the way to treat the landscape water[8]. In the previous research, the pump was arranged by experience to increase the flow rate of landscape water, but it is difficult to optimize the setting. Therefore, in this paper, we use the hydrodynamic model to conduct a computer simulation of the landscape water system[9], In order to provide a scheme for the hydrodynamic optimization design in practice.

1. Project overview

The overall shape of the Moon Bay presents the east-west direction, the underwater terrain distribution has no obvious rules, and the water flow in the bay is slow, the water exchange activity

is poor, and the water flow rate is low, which is prone to the problem of water quality deterioration. The above problems are solved by designing the water system hydrodynamic enhancement pump system to improve the flow rate.

2. Hydrodynamic model

2.1 The Basic Eq

$$\frac{\partial \xi}{\partial t}+\frac{\partial p}{\partial x}+\frac{\partial q}{\partial y}=0$$

$$\frac{\partial p}{\partial t}+\frac{\partial}{\partial x}(\frac{\partial p^2}{h})+\frac{\partial}{\partial y}(\frac{pq}{h})+gh(\frac{\partial \xi}{\partial x})+\frac{gp\sqrt{p^2 2+q^2}}{C^2h^2}-\Omega q-f(V)V_x=0$$

$$\frac{\partial p}{\partial t}+\frac{\partial}{\partial x}(\frac{\partial p^2}{h})+\frac{\partial}{\partial y}(\frac{pq}{h})+gh(\frac{\partial \xi}{\partial y})+\frac{gp\sqrt{p^2 2+q^2}}{C^2h^2}-\Omega q-f(V)V_y=0$$

Where x and y are the spatial coordinates, t is the time, h is the water depth, ξ is the free water level, p, q are the flow density in x and y directions, c is the Chezy resistance coefficient, g is the gravity acceleration, f (V) is the wind friction factor, V and Vx, VyIs the wind speed and the wind speed component in the x and y direction, Ω, is the Coriol coefficient[10].

2.2 Establishment of the Moon Bay model

The water area of Moon Bay is divided into two independent waters by north ditch. In order to facilitate calculation and choose the best design scheme, the two areas of Moon Bay are analyzed and calculated separately, as shown in Figure 1.

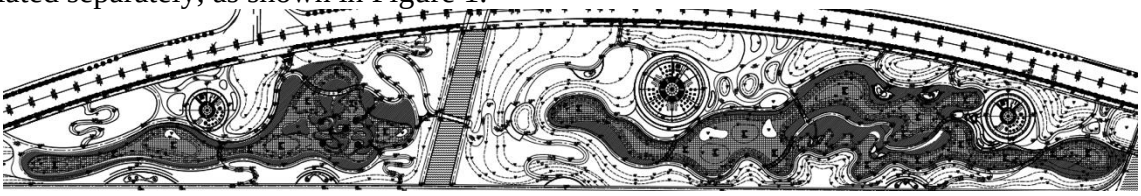

Figure 1: Topographic map of Moon Bay

Turn the north and south topographic maps into the CAD topographic map and then select the boundary points and internal points. The boundary data and elevation data were extracted, the xyz files were converted separately, imported into MIKE zero, and the grid was drawn, as shown in Figure 2 and 3.

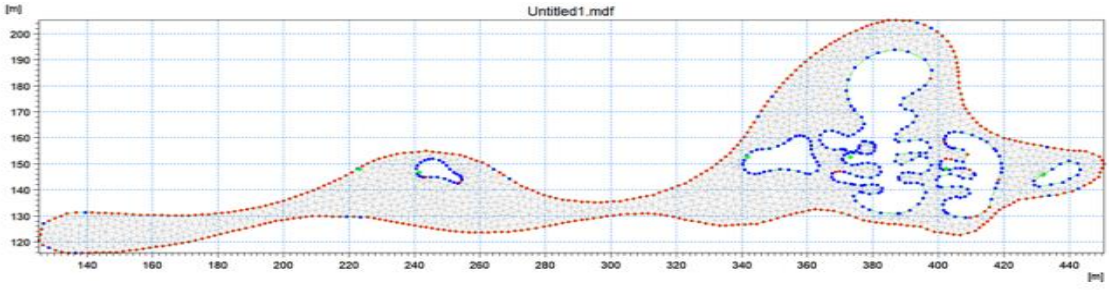

Figure 2: Topographic grid section (North area)

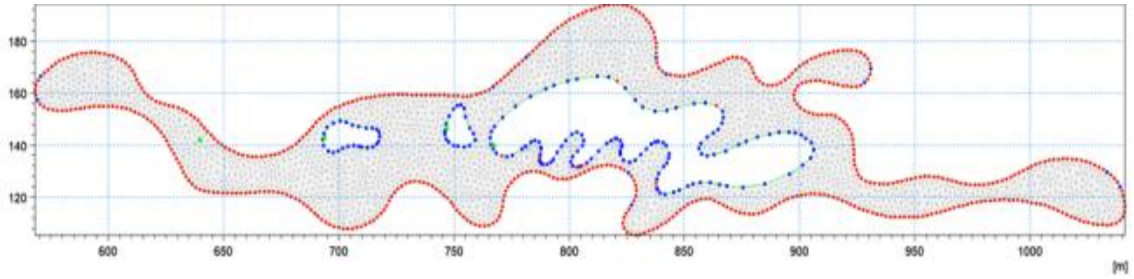

Figure 3: Topographic grid section (South area)

Model running time setting: the selected model running time starts 00:00:00 on January 1, 2023 and runs until 5:00:00 on January 1, 2023. The total time was 5 hours with time steps of 36s and 500 steps. The imported topographic data is shown in the Figure 4 and 5 below.

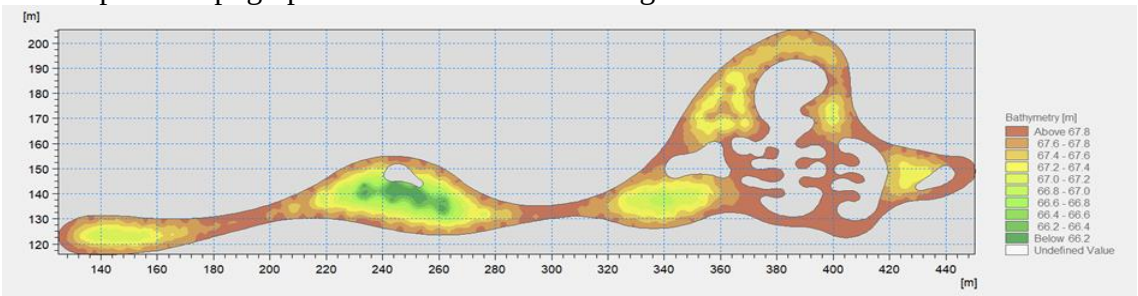

Figure 4: North-side area topographic data

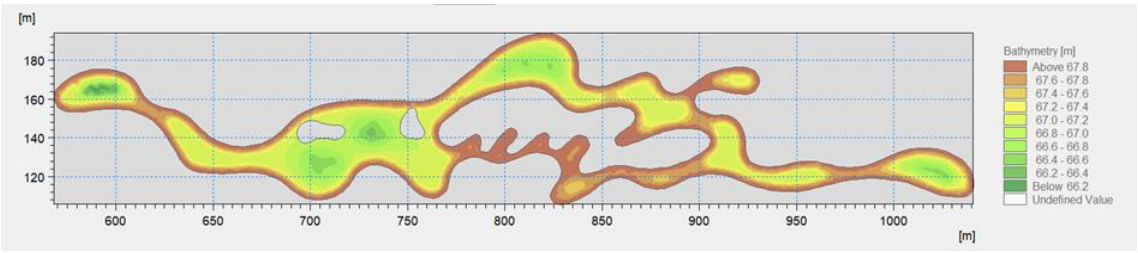

Figure 5: Topographical data of the south side area

When establishing the model, the flow rate provided by the pump is converted into the flow rate of boundary conditions (Table 1, Table 2, Table 3, Table 4, Table 5, and Table 6) to facilitate analysis and calculation. Firstly, the boundary model is established, as shown in Figure 6 and Figure 7.

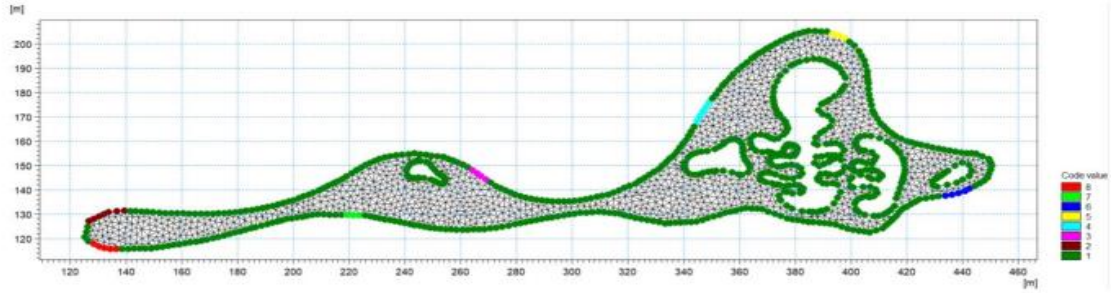

Figure 6: Distribution diagram of boundary setting (north side area)

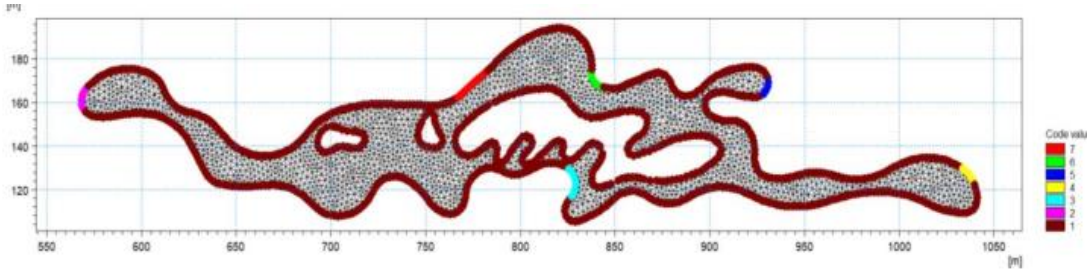

Figure 7: Border Settings Distribution Map (South Area)

2.3 Determine the simulation scheme

We observe the topographic distribution of Moon Bay, compare the position and number of inlet and outlet respectively, and finally determine three sets of distribution schemes [11], as shown in Figure 8-10 and Table 1-6.

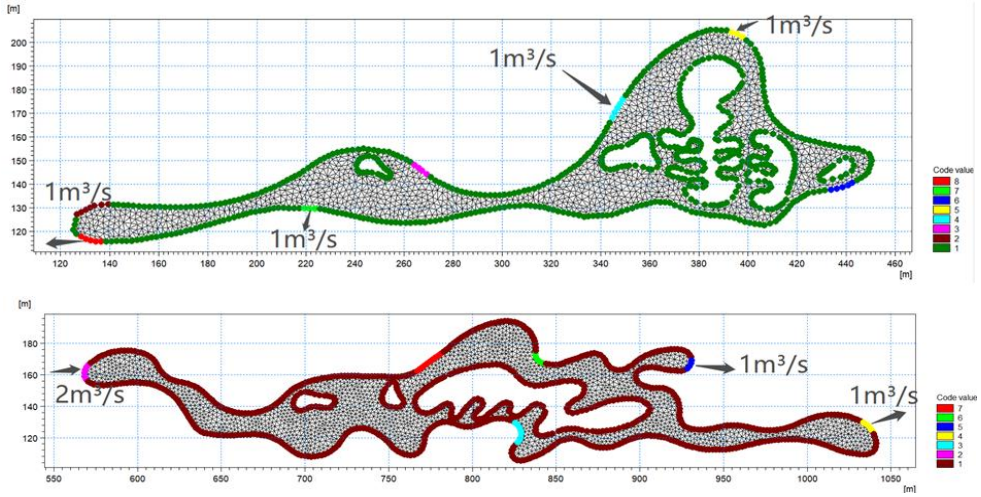

Figure 8: Scheme 1

Table 1: Scheme setting of the northern area boundary

Boundary number	Water intake / water outlet	Flow rate (m ³/ s)
4	water penetration	1
5	water penetration	1
7	yielding water	1
8	yielding water	1

Table 2: Scheme 1 The boundary scheme setting of the south area

Boundary number	Water intake / water outlet	Flow rate (m ³/ s)
2	yielding water	2
4	water penetration	1
5	water penetration	1

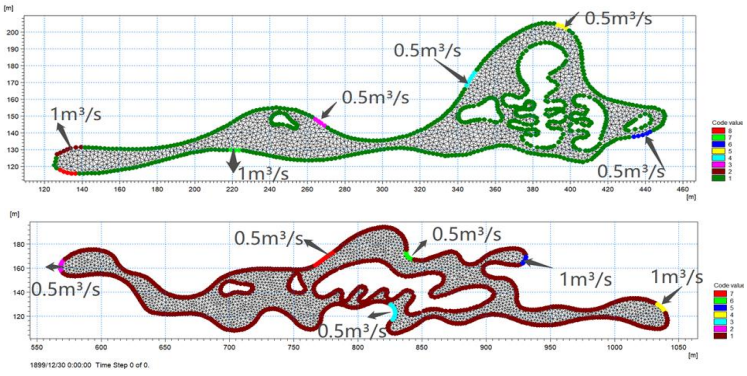

Figure 9: Scheme 2

Table 3: Scheme setting on the northern regional boundary side of Scheme II

Boundary number	Water intake / water outlet	Flow rate (m ³/ s)
2	yielding water	1
3	water penetration	0.5
4	water penetration	0.5
5	water penetration	0.5
6	water penetration	0.5
7	yielding water	1

Table 4: Scheme 2 Border scheme setting of the south area

Boundary number	Water intake / water outlet	Flow rate (m ³/ s)
2	yielding water	0.5
3	yielding water	0.5
4	water penetration	1
5	water penetration	1
6	yielding water	0.5
7	yielding water	0.5

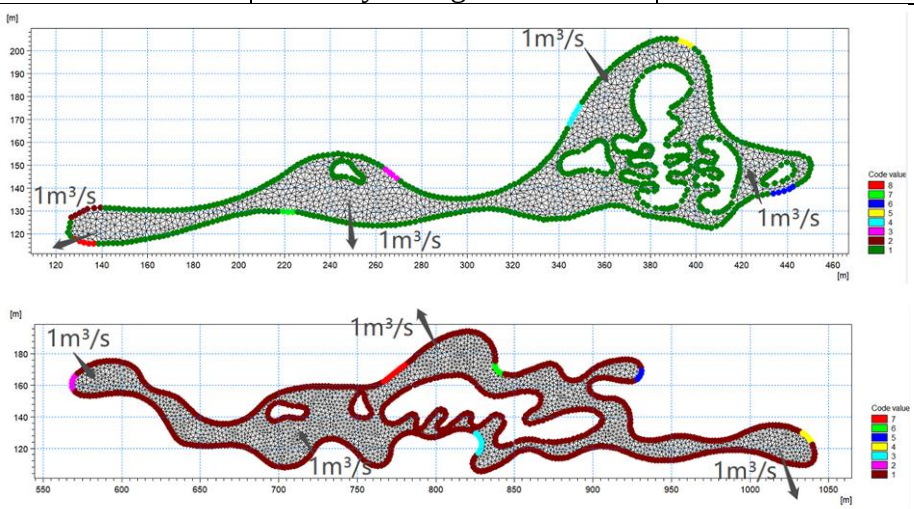

Figure 10: Scheme 3

Table 5: Scheme setting of the three north region boundary

number	Water intake / water outlet	Flow rate (m ³/ s)	abscissa (m)	ordinate (m)
1	yielding water	1	140	120
2	yielding water	1	250	130
3	water penetration	1	360	190
4	water penetration	1	424	150

Table 6: Setting of the south area boundary scheme

number	Water intake / water outlet	Flow rate (m ³/ s)	abscissa (m)	ordinate (m)
1	yielding water	1	580	165
2	yielding water	1	720	130
3	water penetration	1	820	180
4	water penetration	1	1020	120

3. Results and Discussion

The simulation results of the south side hydrodynamic model are shown in the figure below [12]

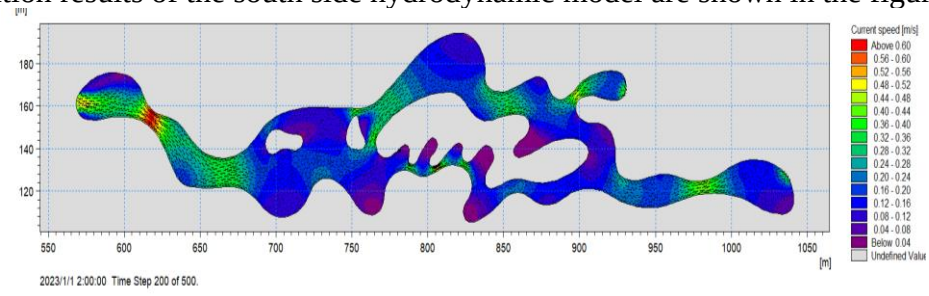

Figure 11: Schematic diagram of water flow rate distribution at the second hour

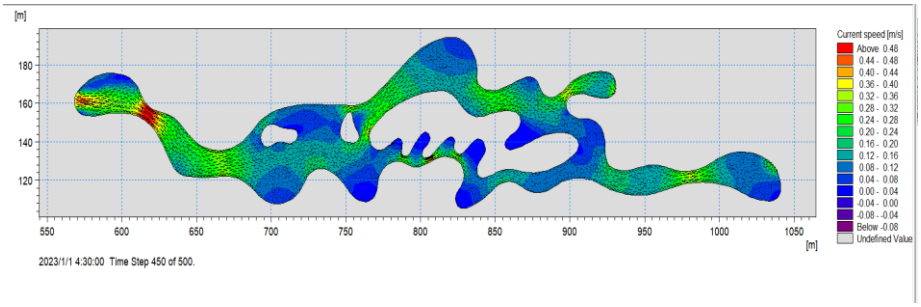

Figure 12: Schematic distribution of flow rate at 4.5 hours

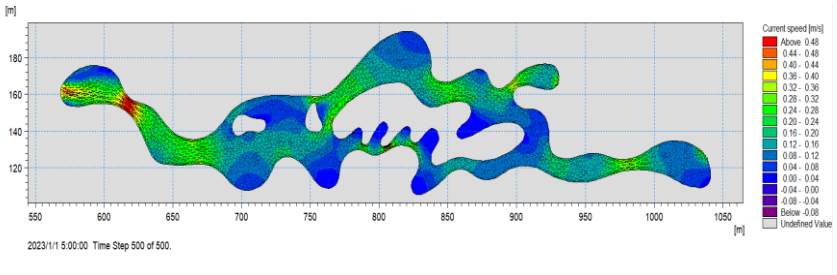

Figure 13: The distribution of water flow rate at the fifth hour

Compared with Figure 11 and Figure 13, the flow field indicates that the flow field has not reached the stable state; for the comparison between Figure 12 and Figure 13, the flow field is basically consistent and the flow field is stable, so the flow field characteristics are analyzed in combination with the simulation results of the fifth hour.

3.1 Simulation results of the hydrodynamic model

3.1.1 Simulation results of scheme hydrodynamic model

The maximum flow rate in the north area of Scheme 1 is 0.44m / s, the flow rate exceeding 0.3m / s is less than 10%, and the flow field is relatively small overall. The water flow basically follows the flow from south to north direction. Flow velocity is lower at broad east-west distances and relatively high at narrower locations[13]0, as shown in Figure 14 and 15.

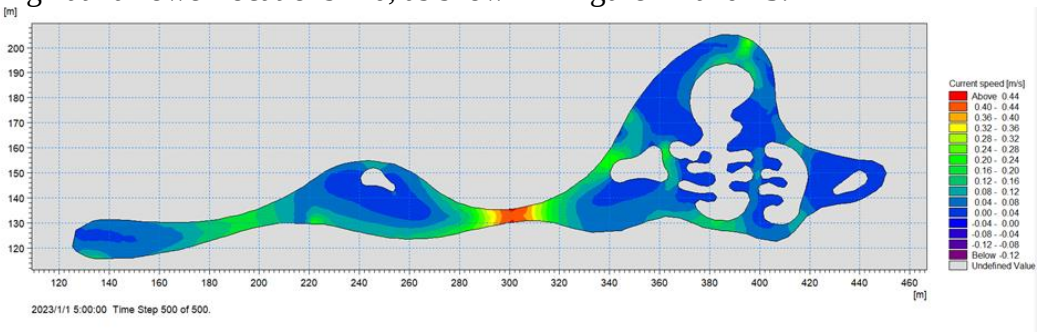

Figure 14: Schematic distribution of flow rate in the fifth hour

The maximum flow rate in the south area is 0.48 m/s, and the flow rate exceeding 0.3m / s is less than 30%. The water flow basically follows the flow direction from north to south. Flow velocity is lower at wide east-west distances and higher at narrow east-west distances.

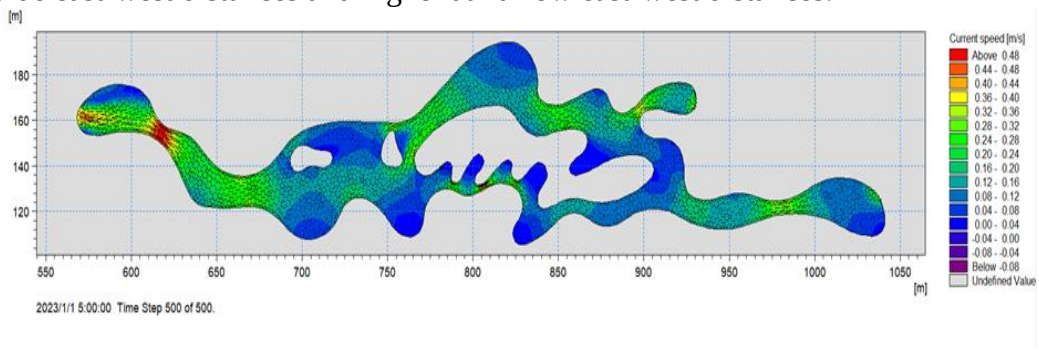

Figure 15: Distribution of water flow rate at the fifth hour

3.1.2 Simulation results of Scheme 2 hydrodynamic model

The maximum flow rate in the north area of scheme 2 is 0.375m / s, the flow rate exceeding 0.3m / s is less than 10%, and the flow field is relatively small overall. The water flow basically follows the flow from south to north direction. Flow velocity is lower at broad east-west distances and relatively high at narrower locations, as shown in Figure 16 and 17.

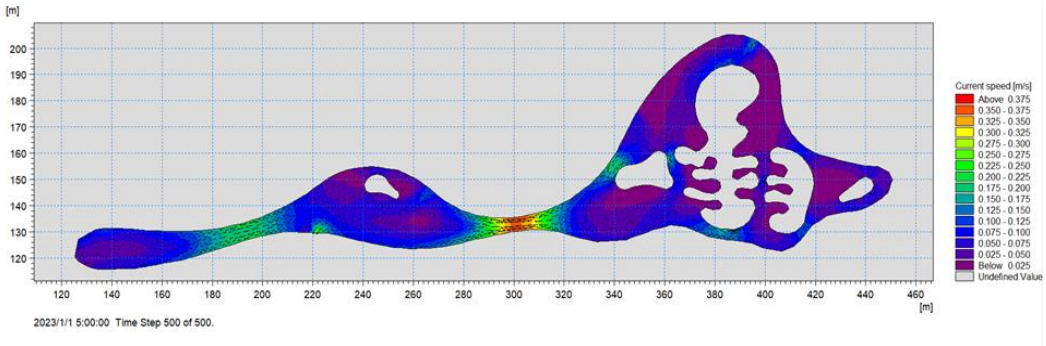

Figure 16: Schematic diagram of water flow rate distribution at the fifth hour

The maximum velocity in the south area of Scheme 2 is 0.44 m/s, and the velocity exceeding 0.3m/s is less than 20%. The water flow basically follows the flow from south to north direction. Flow velocity is lower at wide east-west distances and higher at narrow east-west distances.

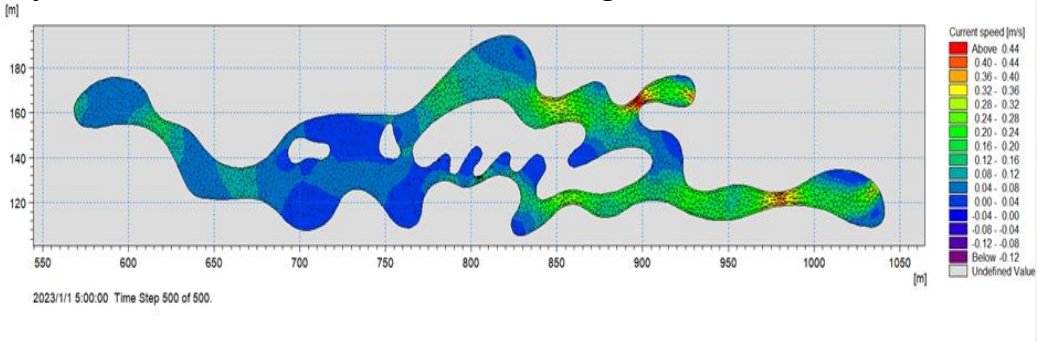

Figure 17: Distribution of water flow rate at the fifth hour

3.1.3 Scheme three hydrodynamic model simulation results

The maximum flow rate of the north area of scheme 3 is 1.50m / s, about 50% of the flow rate exceeds 0.3m / s, and about 70% of the area flow rate exceeds 0.1m / s. Compared with scheme 1 and scheme 2, the overall effect is also significantly improved. The water flow basically follows the flow from south to north direction. Flow velocity is lower at broad east-west distances and relatively high at narrower locations[14], as shown in Figure 18 and 19.

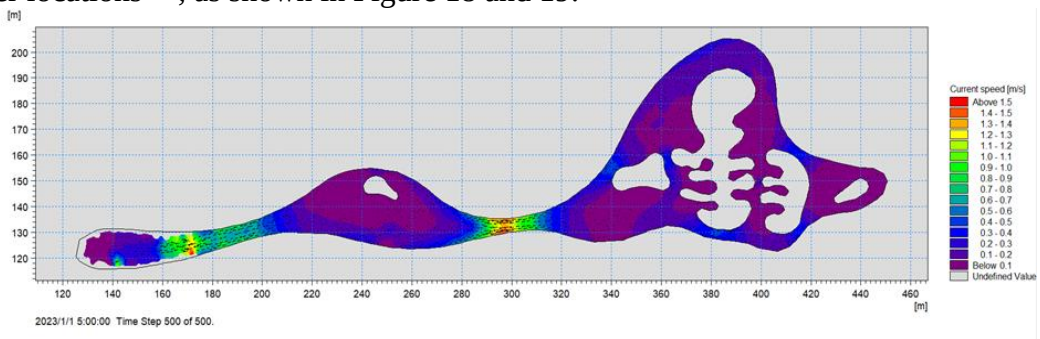

Figure 18: Distribution of water flow rate at the fifth hour

The maximum flow rate in the south area of Scheme 3 is 1.80 m/s, and the flow rate exceeding 0.3m / s is less than 20%. The flow rate of the flow field is small, and a small area of the water flow is promoted, still does not participate in the circulation.

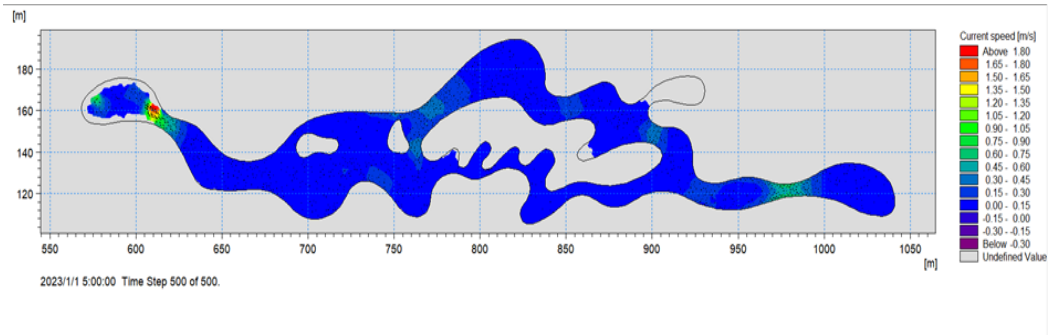

Figure 19: The distribution of water flow rate at the fifth hour

3.1.4 The best scheme determined by the hydrodynamic model

Where the maximum flow velocity exceeds 0.44 m/s and less than 10% exceeds 0.3 m/s; the maximum flow velocity exceeds 0.48 m/s and the flow velocity exceeds 0.3 m/s is less than 30%.

If the maximum flow velocity exceeds 0.375 m/s and the area is less than 10%, the maximum flow velocity exceeds 0.44 m/s and the flow velocity exceeds 0.3m/s is less than 20%[15].

The maximum flow rate on the north side of the scheme 3 exceeds 1.50 m/s; the area is about 50%, and the water flow rate is over 0.1 m/s; the maximum flow rate in the south side exceeds 1.80m/s, and the water flow rate in most areas is lower than 0.15m/s.

By comprehensively comparing the flow rate of the three schemes, the scheme 1 in the south area and the north area adopt scheme 3 as the optimal scheme.

4. Conclusion

This paper designs the scheme of MIKE and predicts the flow velocity. Based on the model operation results of the three schemes, the following conclusions are obtained:

The hydrodynamic model is established by MIKE 21 to predict the flow rate under different schemes. The maximum flow rate in the south area exceeds 0.48 m/s and the flow rate exceeds 0.3 m/s is about 30%; that the maximum flow rate in the north area exceeds 1.50m/s compared with Scheme 1 and Scheme 2, about 50% of the flow rate is more than 0.30 m/s, exceeding 0.3m/s can maintain the virtuous cycle of urban water ecosystem, and the overall effect is significantly improved compared with Scheme 1 and Scheme 2, and about 70% of the regional water flow rate exceeds 0.1m/s.

By comprehensive comparison, it can be seen that the selection scheme of the north area and the south area have the best effect on improving the overall flow rate and can be used as the best scheme.

References

[1] Li Jin. Current situation and treatment technology of urban landscape water pollution [J]. Heilongjiang Science, 2021, 12 (18): 157-159.

[2] Su Lifeng. Discussion on the application of micro-nano bubble technology in landscape water treatment [J]. Urban and rural construction, 2020 (11): 72-74.

[3] Wu Guorong. Case of high standard landscape water design with underground air flotation and biological filtration [J]. Water purification technology, 2021, 40 (12): 147-155.

[4] Gao Wenqi. Application of microflocculation and filtration process in water treatment of building landscape [J]. China Building Materials Technology, 2016, 25 (02): 59-60.

[5] Hu Zhongbang. Application of an embedded control system in landscape water treatment [J]. Journal of Hangzhou Electronic Technology University, 2014, 34 (03): 99-102.

[6] Liu Haiyan. Analysis and application of landscape water treatment technology of nanoscale activated carbon fiber [J]. Examination Weekly, 2013 (83): 193-194.

[7] Zhang Jun, Tong Ningjun, Chen Xu, Pan Junbiao. Application of the EW-MP microbial purification of ecological water treatment system in the field of landscape water treatment [J]. Chinese Horticultural Digest, 2011, 27 (08): 188-189.
[8] Li Qianqian. Effect of flow velocity on the apparent pollution of urban landscape water bodies [D]. Suzhou University of Science and Technology, 2017.
[9] Yao Jian. On the construction of MIKE11 hydrodynamic model [J]. Heilongjiang Water Conservancy Technology, 2022, 50 (10): 86-89
[10] Xu Ting. Overview and application of the Danish MIKE21 model [J]. Water Conservancy Technology and Economy, 2010, 16 (08): 867-869.
[11] Zhu Yiping, Zhang Haiping, Chen Ling. Hydrodynamic optimization design of landscape water bodies [J]. Water supply and drainage in China, 2007 (10): 36-38.
[12] Deng Yixiang, Zhang Aijun. Research status and prospect of numerical simulation of environmental hydrodynamics [J]. Resource Development and market, 1998 (06): 276-278.
[13] Wang Jiang, Zhang Peng. Study on the velocity distribution of flood flow field in Tianjing Lake area based on MIKE212 D hydrodynamic model [J]. Zhi Huai, 2023 (01): 22-24.
[14] Wang Jianping, Su Baolin, Jia Haifeng, et al. Study on model system of Miyun Reservoir and its watershed [J]. Environmental Science, 2006, 27 (7): 1286-1291.
[15] Li Yafeng, Wu Jianbo, Cheng Hao. Simulation of pollutant diffusion in Tanghe Reservoir based on EFDC model [J]. Journal of Shenyang Architecture University, 2022, 38 (05): 945-952.